JOURNAL OF MATERIALS SCIENCE **36** (2001) 329–333

# Selective area MOVPE growth for 1.55 $\mu$m laser diodes with vertically tapered thickness waveguide

HYUN-SOO KIM*
*Department of Material Science and Engineering, Korea University, Anam-dong 5-1, Sungbuk-ku, Seoul 136-701, South Korea*
*E-mail: kimhyunsoo@hanmail.net*

DAE KON OH, MOON-HO PARK, NAM HWANG
*Electronics and Telecommunications Research Institute, Yusong P.O.Box 106, Taejon 305-600, South Korea*

IN-HOON CHOI
*Department of Material Science and Engineering, Korea University, Anam-dong 5-1, Sungbuk-ku, Seoul 136-701, South Korea*

We investigated the influence of growth pressure and V/III ratio on selectively grown InGaAs/InGaAsP MQW by using low-pressure metalorganic vapor phase epitaxy (MOVPE). Diffusion parameters were determined from curve fitting to experimental data by using the diffusion equation. The diffusion length decreased with the increase of growth pressure. The growth enhancement at the center of the mask opening increased and saturated over growth pressure of 100 mbar. The uniformity of PL intensity along the lateral direction was improved with the decrease of growth pressure and V/III ratio. We also realized a 1.55 $\mu$m SSC-LD with vertically tapered thickness waveguide. The device exhibited a far field angle of $6.9^\circ \times 12.4^\circ$ and a slope efficiency as high as 0.31 W/A.


## 1. Introduction

Selective area metalorganic vapor phase epitaxy (MOVPE) is a promising technique for fabricating monolithic integrated devices such as modulator-integrated DFB LD [1], integrated optical transmitters [2] and LD-gate switch [3], because mask width controls locally the growth rate and material composition which makes in-plane bandgap control possible in a single growth step. It is well known that growth enhancement is induced by lateral diffusion of source material from the mask region to the unmasked region (epilayer region) [4]. Lateral diffusion in MOVPE generally consists of gas phase diffusion and surface migration on the mask [5]. It was reported that growth enhancement as well as PL wavelength of selectively grown InGaAs(P) bulk layer has been changed by the variation of growth pressure [6], which indicates that diffusion length is strongly affected by growth pressure.

In this paper, we investigated the influence of growth pressure and V/III ratio on the growth enhancement and lateral uniformity of selectively grown InGaAs/InGaAsP MQW layer by using low pressure MOVPE. We also fabricated a 1.55 $\mu$m spot size converter integrated laser diode (SSC-LD) with vertically tapered thickness waveguide.

## 2. Experimental

The selective area growth was performed in an AIX 200/4 system with a horizontal gas flow. The growth temperature was fixed at 650 °C. The growth pressure was changed from 30 to 300 mbar. Typical growth rate on unmasked substrate was 1 $\mu$m/h for InP, 1.2 ∼1.3 $\mu$m/h for InGaAsP and 1.75 $\mu$m/h for InGaAs. The total $H_2$ gas flow rate was around 12.5 slm. The precursors for group III and V were trimethylindium (TMIn), trimethylgallium (TMGa), arsine ($AsH_3$) and phosphine ($PH_3$). The SiN*x* films were used as the masks for selective area growth. The masks for the selective area growth were 200 nm thick $SiN_x$ film deposited on (100) exactly-oriented sulfur-doped InP substrate by using plasma enhanced chemical vapor deposition (PECVD) and patterned by conventional photolithography. The stripe direction was aligned to [011]. Before the growth, the patterned substrate was slightly etched for 30 second by $3H_2SO_4 : H_2O_2 : H_2O$ solution.

* Author to whom all correspondence should be addressed.

A 0.2 $\mu$m thick n-InP buffer layer was grown for improved crystal quality. The MQW layer consisted of five pairs of 35 Å-thick InGaAs quantum well and 100 Å-thick lattice-matched InGaAsP barrier ($\lambda_g = 1.32$ $\mu$m) surrounded by 500 Å-thick InGaAsP ($\lambda_g = 1.25$ $\mu$m) separated confinement heterostructure (SCH) layer. On the top of upper SCH layer, a 0.5 $\mu$m thick p-InP cladding ($N_a = 5 \times 10^{17}\text{cm}^{-3}$) layer was grown. The thickness of the selectively grown layers was measured by an alpha-step and scanning electron microscopy (SEM). The photoluminescence (PL) measurements of the selectively grown layers were carried out at room temperature using a He-Ne laser with 5 $\mu$m diameter.

## 3. Results and discussion

### 3.1. Growth pressure dependence

In recent years, several models for MOVPE have been developed with the intention to analyze selective area growth [7–10]. Different surface features of the substrate are created by utilizing dielectric masks. In most cases, it is considered that surface migration can be negligible as compared to gas phase diffusion [8–10]. However, we discuss on growth pressure dependence of growth enhancement based on the general model by Fujii *et al.* [7]. The differential equation governing the crystal growth is based on the mass preservation of the species involved. The diffusion of growing species is described by the differential equation as following,

$$\frac{\partial n}{\partial t} = (D^{\text{surf}} + D^{\text{gas}})\frac{d^2 n(x)}{dx^2} + J_o - Kn(x) - Gn(x)$$
$$= \bar{D}\frac{d^2 n(x)}{dx^2} + J_o - \frac{n(x)}{\tau} \tag{1}$$

where $K$ and $G$ are the desorbing probability and growing probability per unit time of surface source materials. $D^{\text{surf}}$ and $D^{\text{gas}}$ are diffusion constant of surface migration and gas phase diffusion. $J_o$ is the source supply per unit time from the gas phase.

Where we introduced the overall diffusion coefficient

$$\bar{D} = (D^{\text{surf}} + D^{\text{gas}})$$

and the lifetime

$$\tau = \frac{1}{(K+G)} \tag{2}$$

In the steady state $\partial n/\partial t = 0$, so that Equation 1 leads to

$$\frac{n(x)}{\tau} = J_o + \bar{D}\frac{d^2 n(x)}{dx^2} \tag{3}$$

In case of patterned substrates, the mask (index M) and the epilayer region (index E) between the masks are considered as regions of homogeneous surface features so that for each region, the differential Equation 3 has to be defined by the respective material parameters, $\bar{D}_E$, $\tau_E$ and $\bar{D}_M$, $\tau_M$. By introducing the normalized concentrations $\bar{n}_E(x) = n_E(x)/(\tau_E J_o)$ on the open region

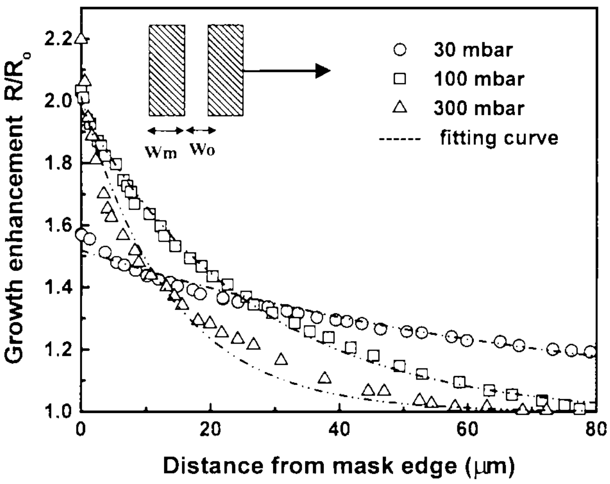


*Figure 1* Lateral growth enhancement profile of MQW grown under various growth pressure ($W_o = 20$ $\mu$m, $W_m = 100$ $\mu$m). The dot line is a fitting curve using Equation 8.

and $\bar{n}_M(x) = n_M(x)/(\tau_M J_o)$ on the mask, where $\tau_E J_o$ is the concentration at a planar substrate, we obtain the following equations:

$$\frac{\bar{n}_E(x)}{L_E^2} = \frac{1}{L_E^2} + \frac{d^2\bar{n}_E(x)}{dz^2}$$
$$\frac{\bar{n}_M(x)}{L_M^2} = \frac{\tau_E^M}{L_M^2} + \frac{d^2\bar{n}_M(x)}{dz^2} \tag{4}$$

with the effective diffusion lengths of source materials

$$L_E = \sqrt{\bar{D}_E\tau_E} \quad \text{and} \quad L_M = \sqrt{\bar{D}_M\tau_M} \tag{5}$$

and the lifetime ratio between the mask and open regions

$$\tau_E^M = \frac{\tau_M}{\tau_E} \tag{6}$$

The boundary conditions require continuos concentration and continuous diffusion flux of source material at the boundaries:

$$\bar{n}_E(x)|_{\text{interface}} = \bar{n}_M(x)|_{\text{interface}}$$
$$\bar{D}_E\frac{d}{dz}\bar{n}_E(x)\Big|_{\text{interface}} = \bar{D}_M\frac{d}{dz}\bar{n}_M(x)\Big|_{\text{interface}} \tag{7}$$

The diffusion length $L_E$ and $L_M$ and the lifetime ratio $\tau_E^M$ are parameters which can be determined by curve fitting to experimental data as will be discussed below.

Fig. 1 shows the lateral growth enhancement profiles for InGaAs/InGaAsP MQW-DH structures grown under different growth pressure. As shown in Fig. 1, the growth enhancement profile was influenced drastically by growth pressure, and the region affected by gas phase diffusion increased as growth pressure decreased. When diffusion length is much less than the open region width, growth enhancement ($R(x)/R_o$) in

TABLE I Values of diffusion parameters as a result of curve fitting

| Growth pressure (mbar) | $L_E$ | $L_M$ | |
|---|---|---|---|
| 30 | 74.5 | 150 | 2.84 |
| 100 | 25 | 120 | 4.94 |
| 300 | 13.7 | 85 | 6.0 |

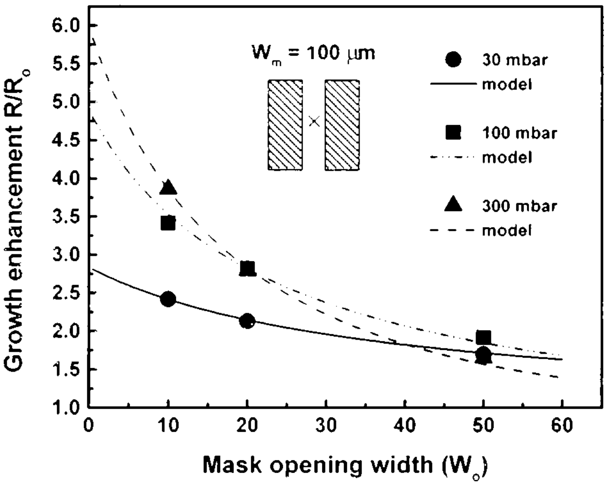


*Figure 2* Growth enhancement of selectively grown MQW as a function of mask opening width ($W_o$).The thickness was measured at the center of the mask opening.

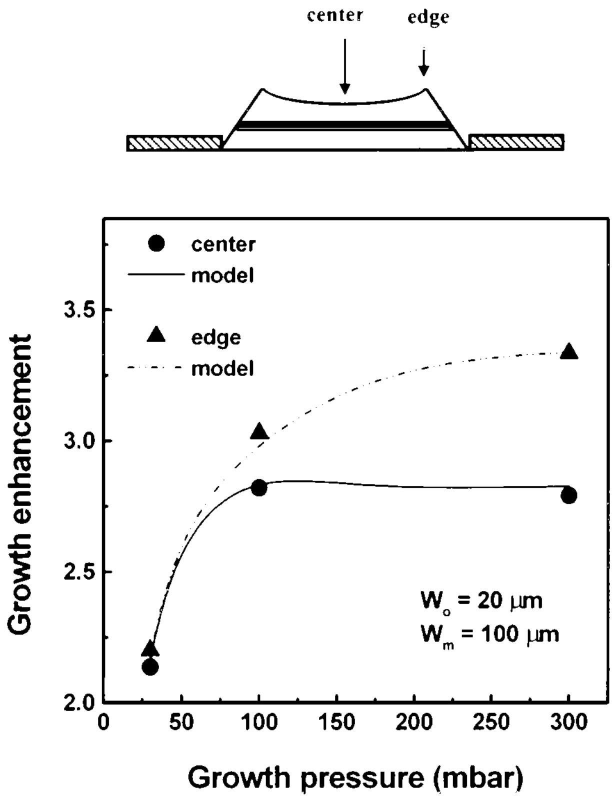


*Figure 3* Growth enhancement measured at the center of the mask opening and at the mask edge.

the open region is expressed as following [11]

$$\frac{R(x)}{R_o} = \left(\frac{R_E - R_o}{R_o}\right)\mathrm{Exp}\left(-\frac{x}{L^E}\right) + 1 \qquad (8)$$

where $L^E$ is the diffusion length in epilayer region, $R_o$ is growth rate in unmasked region and $R_E$ is growth rate at mask edge. Gas phase diffusion length was obtained by curve fitting to lateral growth enhancement distribution by using the Equation 8. As shown in Table I, gas phase diffusion length was inverse proportional to growth pressure. The influence of growth pressure on the relations between growth enhancement and mask opening is shown in Fig. 2. The growth enhancement generally increased with the decrease of mask opening width, because the laterally supplied material is distributed over a smaller area of epitaxial growth. The dependence of growth pressure on growth enhancement increased with decreasing the mask opening width. In addition to the growth enhancement at the center $R_C/R_o$, those measured at the edge $R_E/R_o$ are displayed in Fig. 3. The growth enhancement at mask edge increased with the growth pressure. However, the growth enhancement at the center of the mask opening increased and saturated with increase of growth pressure. The saturation of growth enhancement at 300 mbar was observed due to polycrystalline deposition on mask. Chemical reaction at the mask surface reduced the gas phase concentration of group III source materials. The growth enhancement difference between center and edge increased with increasing the growth pressure due to the suppression of gas phase diffusion length. By fitting the model to the experimental data in Fig. 2 and Fig. 3, we obtained the diffusion parameters as shown in

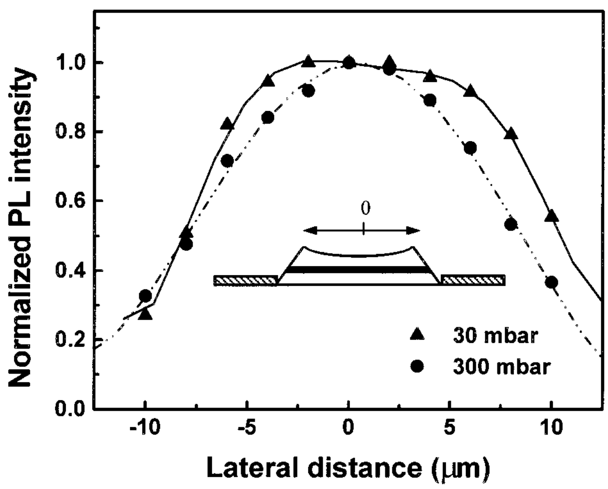


*Figure 4* Normalized PL intensity distribution of selectively grown MQW layer under different growth pressures. The arrow in the insert represents the measurement direction ($W_o = 20\ \mu$m, $W_m = 100\ \mu$m).

Table I. The shape of growth enhancement distribution was strongly dependent on $L_E$ and $L_M$, and the maximum growth enhancement was strongly dependent on the lifetime ratio. Fig. 4 shows lateral PL intensity profile of selectively grown MQW layer under different growth pressure. The MQW grown under 30 mbar has a higher lateral uniformity compared to that under 300 mbar. This result is explained as following. As shown in Fig. 3, the difference of growth enhancement between mask edge and mask opening center increased as growth pressure increased. Thus, the lateral thickness uniformity is degraded as growth pressure increased.

TABLE II The V/III ratio of InGaAs/InGaAsP MQW SCH structure

| | MQW#1 | MQW#2 |
|---|---|---|
| InGaAS QW | 13.8 | 4.5 |
| InGaAsP barrier | 190 | 65 |

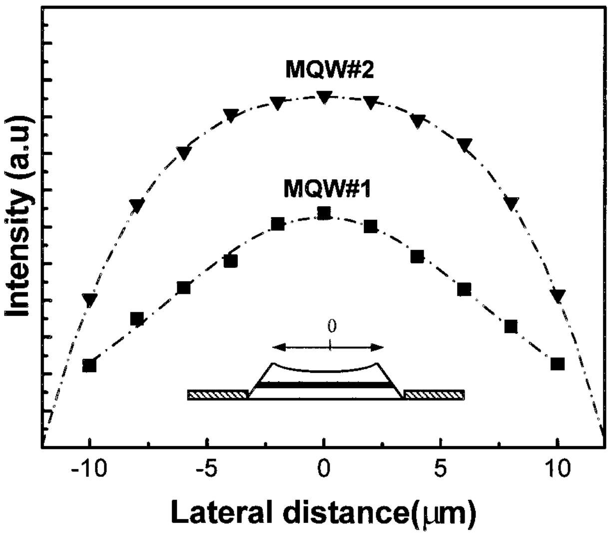


*Figure 5* PL intensity distribution of selectively grown MQW layer under different V/III ratios ($W_o = 20$ μm, $W_m = 100$ μm).

## 3.2. Effect of V/III ratio

Fig. 5 shows lateral PL intensity profile of selectively grown MQW under different V/III ratios. The MQW grown under low V/III ratio has a higher PL intensity and lateral uniformity compared to that grown under high V/III ratio. This result was explained as following. Sakata *et al*. reported that gas phase diffusion length of InGaAs(P) increased with decreasing the V/III ratio [12]. The high partial pressure of group V hydrides would result in the enhanced decomposition rate of group III species, such decomposed species tend to easily incorporate with group V atoms on the surface, and results in the shorten diffusion length of the species [13]. As a result, lateral uniformity of selectively grown MQW increased as the V/III ratio decreased.

## 3.3. Device application

Spot size converter integrated laser diodes (SSC-LDs), which can achieve low-loss coupling and large alignment tolerance with flat-end fibers or planar lightwave circuits (PLCs), are key devices to promote the development of optical subscriber systems because they can remarkably reduce the module-assembly cost [14]. The MQW active layer and vertically tapered thickness waveguide were grown simultaneously by using an exponentially tapered shape mask as shown in Fig. 6. The properties of the laser diode monolithically integrated with a tapered thickness waveguide depend strongly on the quality of multiple quantum well (MQW) layer and the ratio of the thickness in the LD active region to that in waveguide. Thus, growth pressure was fixed at 100 mbar and V/III ratio was used at same condition of MQW#2 in order to obtain high growth enhancement

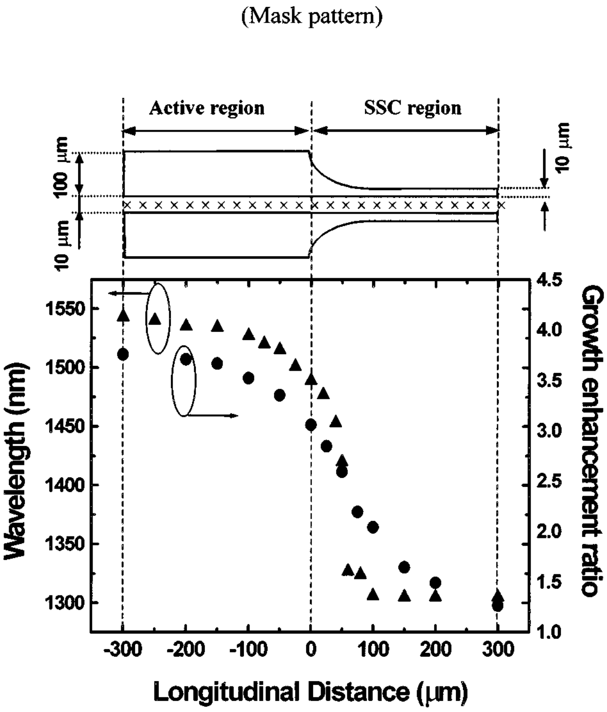


*Figure 6* PL wavelength and growth enhancement profile of selectively grown MQW layer along the longitudinal direction.

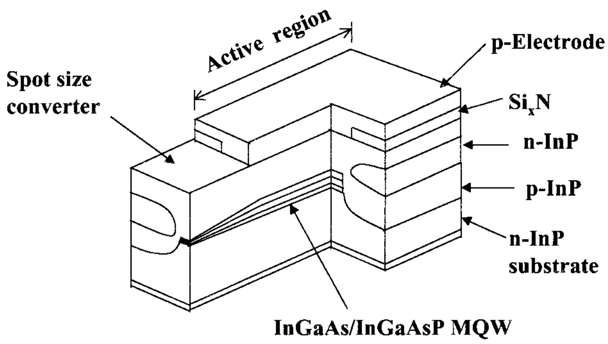


*Figure 7* Schematic diagram of SSC-LD with vertically tapered waveguide.

and improve the quality of the MQW. Fig. 6 shows the growth enhancement (ratio of thickness at the center of the mask opening to that in unmasked region) profile and PL wavelength profile of selectively grown MQW layer through the LD active region to the spot size converter region. The high growth enhancement of about 3.75 at the center of the LD active region was obtained. The PL wavelength profile in the active region is approximately flat and that in the SSC region is gradually shortened as is consistent with the thickness profile. The PL wavelength of MQW layer was changed from 1.55 μm band to 1.3 μm band with a wavelength shift of a 238 nm through the LD active region to the spot size converter region. The transition length, which was defined as 10%–90% of total wavelength shift, was about 135 μm. This profile is suited to reduce the absorption loss of the LD, since the band-gap energy difference between the LD active region and the SSC region is sufficiently large. A schematic structure of SSC-LD with vertically tapered thickness waveguide is illustrated in Fig. 7. The SSC-LD with a pn-buried heterostructure was fabricated by three-step MOVPE growth including

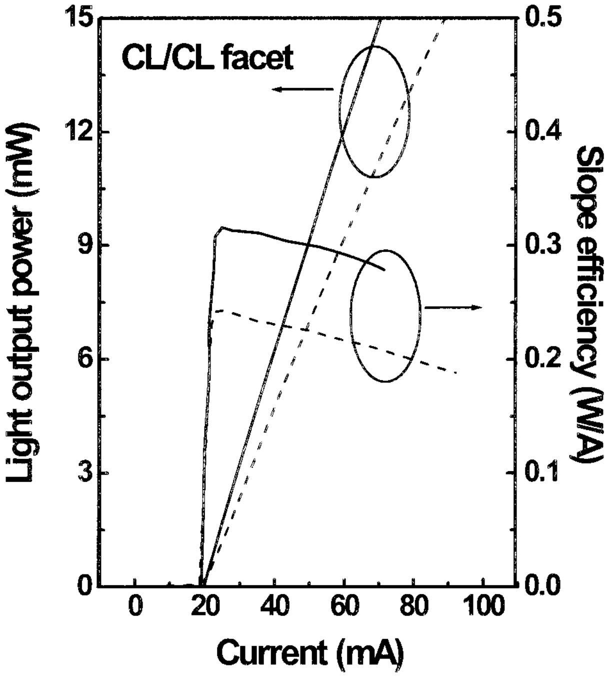


*Figure 8* Light output power versus current curves without facet coating: SSC-LD (solid line) and LD without SSC region (dash line).

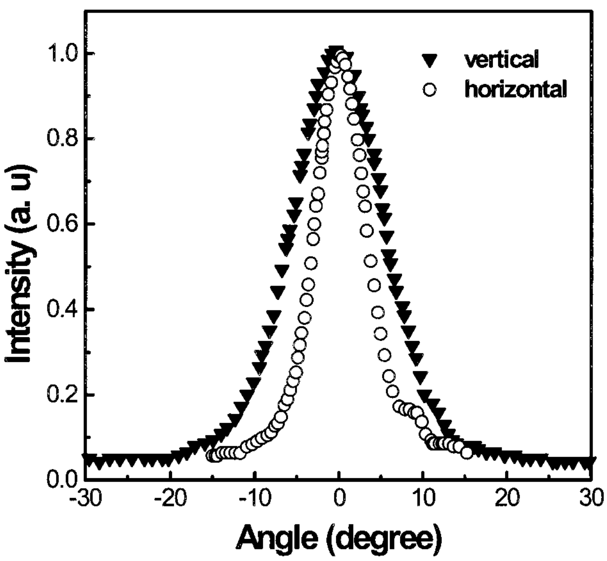


*Figure 9* Far field pattern of SSC-LD in the horizontal and vertical direction.

selective area growth. The LD active region and the SSC region were 300 $\mu$m and 300 $\mu$m-long, respectively. The typical L-I characteristics of SSC-LD without facet coating are shown in Fig. 8. The threshold current of SSC-LD was 19 mA at an ambient temperature of 25 °C. Little increment in threshold current was observed compared with a solitary LD without an SSC region. It indicates that absorption and mode conversion loss in the SSC region were quite small. The SSC-LD exhibited a slope efficiency as high as 0.31 W/A without facet coating. Fig. 9 shows the far field patterns (FFPs) of the SSC-LD. The full width at half maximum (FWHM) of the Gaussian-shaped FFPs without side lobe were 6.9° × 12.4° (horizontal × vertical), and these were about one-third those of LDs without spot-size converter region.

## 4. Conclusion

In conclusion, the influence of growth pressure and V/III ratio on growth enhancement and lateral uniformity of selectively grown InGaAs/InGaAsP MQW was investigated. By fitting theoretical curves to measured growth rate, we determined the diffusion length and lifetime ratio. The uniformity of PL intensity along the lateral direction was improved with the decrease of growth pressure and V/III ratio. We also fabricated a 1.55 $\mu$m SSC-LD with vertically tapered thickness waveguide by selective area MOVPE. The MQW active layer and vertically tapered thickness waveguide were grown at the same time by using an exponentially tapered shape mask. By using these technique, we have successfully realized a very narrow beam divergence and a high slope efficiency without facet coating.

## References


1. M. AOKI, M. SUZUKI, M. TAKAHASHI, H. SANO, T. IDO, K. KAWANO and A. TAKAI, *Electron. Lett.* **28** (1992) 1157.
2. T. TAKEUCHI, T. SASAKI, M. HAYASHI, K. HAMAMOTO, K. MAKITA, K. TAGUCHI and KO. KAOMATSU, *IEEE Photon. Tech. Lett.* **8** (1996) 361.
3. E. LACH, G. LAUBE, M. SCHILLING, A. AMBROSY, J. HEHMANN and L. DEMBECK, in Proceedings of the ECOC'95, Brussels (1995) p. 111.
4. K. YAMAGUCHI and K. OKAMOTO, *Jpn. J. Appl. Phys.* **32** (1993) 1523.
5. T. SASAKI, M. KITAMURA and I. MITO, *J. Cryst. Growth* **132** (1996) 401.
6. T. SASAKI, M. YAMAGUCHI and M. KITAMURA, *ibid.* **145** (1994) 846.
7. T. FUJII and M. EKAWA, *J. Appl. Phys.* **78** (1995) 5373.
8. D. G. CORNONELL and K. F. JENSEN, *J. Cryst. Growth* **114** (1991) 581.
9. M. GIBBON, J. P. STAGG, C. G. CURETON, E. J. THRUSH, C. J. JONES, R. E. MALLARD, R. E. PRITCHARD, N. COLLINS and A. CHEW, *Semiconductor Sci. Technol.* **8** (1993) 998.
10. B. KORGEL and R. F. HICKS, *J. Cryst. Growth* **151** (1995) 204.
11. T. FUJII, M. EKAWA and S. YAMAZAKI, *ibid.* **156** (1995) 59.
12. Y. SAKATA, T. NAKAMURA, S. AE, T. TERAKDADO, Y. INOMOTO, T. TORIKAI and H. HASUMI, *J. Electron. Mater.* **25** (1996) 401.
13. K. KUDO, T. SASAKI and M. YAMAGUCHI, *J. Cryst. Growth* **170** (1997) 634.
14. Y. FURUSHIMA, H. YAMAZAKI, K. KUDO, Y. SAKATA, Y. OKUNUKI, Y. SASAKI and T. SASAKI, *Jpn. J. Appl. Phys.* **38** (1999) 1234.


*Received 28 January*
*and accepted 24 May 2000*